Available online at www.sciencedirect.com

ScienceDirect

Procedia Engineering 191 (2017) 618 – 622

Procedia Engineering

www.elsevier.com/locate/procedia

Symposium of the International Society for Rock Mechanics

New Insights into Fracture Process through In-Situ Acoustic Emission Monitoring during Fatigue Hydraulic Fracture Experiment in Äspö Hard Rock Laboratory

Grzegorz Kwiatek[a,*], Katrin Plenkers[b], Patricia Martínez-Garzón[a], Maria Leonhardt[a], Arno Zang[a], Georg Dresen[a]

[a]*Helmholtz Centre Potsdam, GFZ German Research Centre for Geosciences,Telegrafenberg, Potsdam 14473, Germany*
[b]*GMuG Gesellschaft für Materialprüfung und Geophysik mbH, Bad Nauheim 61231, Germany*

Abstract

In this study we analyze the nano- and picoseismicity recorded during the Fatigue Hydraulic Fracturing (FHF) in situ experiment performed in Äspö Hard Rock Laboratory, Sweden. The fracturing experiment composed of six fractures driven by three different water injection schemes (continuous, progressive and pulse pressurization) was performed during the year 2015 inside a 28 m long, horizontal borehole located at 410 m depth. The fracturing process was monitored with two different seismic networks covering a wide frequency band between 0.01 Hz and 100000 Hz, including broadband seismometers, geophones, high frequency accelerometers and acoustic emission sensors. The combined seismic network allowed for detection and detailed analysis of nearly 200 seismic events with moment magnitudes $M_W < -4$ that occurred solely during the hydraulic fracturing stages. We relocated the seismic catalog using double-difference technique and calculated the source parameters (seismic moment, source size, stress drop, focal mechanism and seismic moment tensor). The derived physical characteristics of induced seismicity are compared with the stimulation parameters as well as with the geomechanical parameters of the site.

Peer-review under responsibility of the organizing committee of EUROCK 2017

Keywords: hydraulic fracturing; acoustic emissions; source parameters; seismic moment tensors

* Corresponding author. Tel.: +49-331-288-1384; fax: +49-331-288-1321.
E-mail address: kwiatek@gfz-potsdam.de

Peer-review under responsibility of the organizing committee of EUROCK 2017
doi:10.1016/j.proeng.2017.05.225

1. Introduction

The geothermic Fatigue Hydraulic Fracturing (FHF) in situ experiment (Nova project 54-14-1) was performed in the Äspö Hard Rock Laboratory/Sweden situated in granitic to dioritic rocks with an age of about 1.8 Ma [1]. The experiment aimed at optimizing geothermal heat exchange in crystalline rock mass by multistage hydraulic fracturing. At a depth of 410 m, six fracture stages were initiated using three different water injection schemes (continuous, progressive and pulse pressurization) inside a 28 m long, horizontal borehole (Figure 1), with up to 30 dm^3 during each fracture stage.

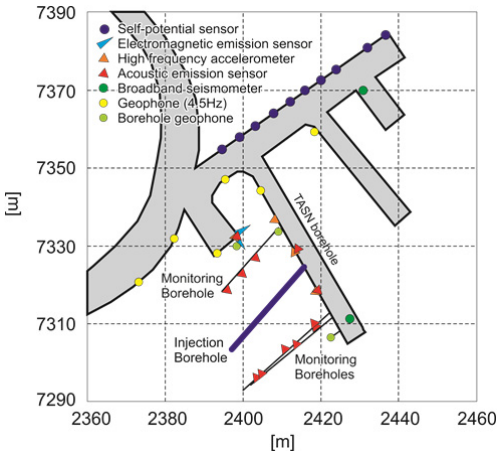

Fig. 1. The map view of all sensors during the hydraulic fracture experiment.

The rock volume surrounding the hydraulic fracturing tests was monitored by three different and independent networks equipped with Acoustic Emission (AE) and accelerometers, short and long-period geophones as well as electromagnetic sensors (Figures 1, 2). The monitored volume was about 30 m x 30 m x 30 m in size. The 16-channel in-situ AE monitoring network manufactured by GMuG [2–5] predominantly used in this study monitored the rupture generation and propagation in the frequency range from 1000 Hz to 100000 Hz using combined 11 acoustic emission sensors and 4 high-frequency accelerometers (1 channel spared for time synchronization between different networks). The acquisition system operated at 1 MHz sampling rate. This monitoring setup was successfully used before [2, 6, 7] to detect and analyze seismic events with rupture dimensions from a few cm- to m-scale [6]. However the environment in Äspö Hard Rock Laboratory was a different one; we had 4-5 Liters/minutes inflow and sensors and equipment had to be adapted to the wet facility. The additional microseismic network covered the lower frequency range from hundreds of hertz to 100 seconds (Figure 2) targeting potentially stronger seismic events. The in-situ AE monitoring system detected and analyzed AE activity in-situ in online mode (P- and S-wave picking, localization). To locate earthquakes, an isotropic velocity model was used. After each stimulation, the results of monitoring were reviewed in order to assess the ongoing microfracturing activity and adjust/improve the monitoring strategy.

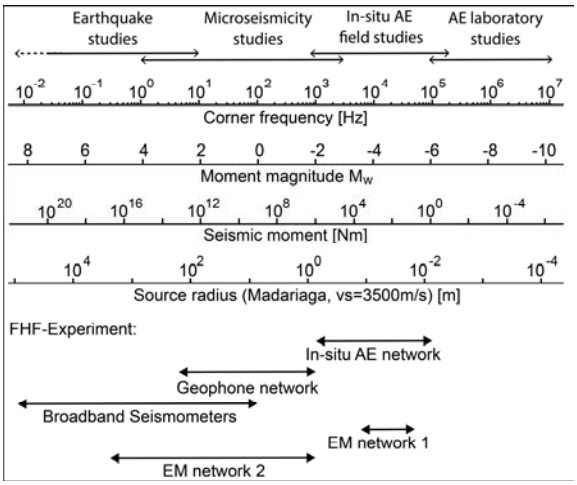

Fig. 2. The frequency ranges of different monitoring networks operating at Äspö Laboratory during FHF experiment.

2. Ongoing data processing

The in-situ AE monitoring network successfully recorded and located 196 earthquakes during most, but not all, hydraulic fractures (HF1, HF2, HF3, HF4 and HF6) (Table 1, Figure 3). In addition, the acquisition system recorded and successfully located approximately 47 events identified later as man-made hammer hits against the tunnel wall (well recorded on high frequency accelerometers and AE sensors). Finally, additional 128 events were identified as working noises and rejected from the analysis. Additional 70 located events could not be clearly determined or attributed to the mentioned signal groups and were rejected as well.

Table 1. Number of events detected, located and relocated in each fracture.

Fracture	Injection style (rock type)	No. AE events	Fluid injected [liter]
HF1	continuous (granodiorite)	49	27.2
HF2	continuous (granodiorite)	102	29.7
HF3	progressive (granodiorite)	16	24.8
HF4	continuous (diorite-gabbro)	1	4.1
HF5	pulse dynamic (diorite-gabbro)	0	14.6
HF6	Conventional (granite)	28	24.2

The initial earthquake catalog was subjected to reprocessing to increase its quality. In the first step, the P- and S-wave picks detected by an automatic algorithm were manually reviewed and refined when necessary. In the following, the earthquakes were relocated (in absolute sense) using updated picks database using the Equivalent Differential Time method [8, 9] and improved velocity model, where additional information on P- and S-wave velocities from ultrasonic velocity measurements as well as iterative comparison of true and estimated hammer hits locations were both taken into account.

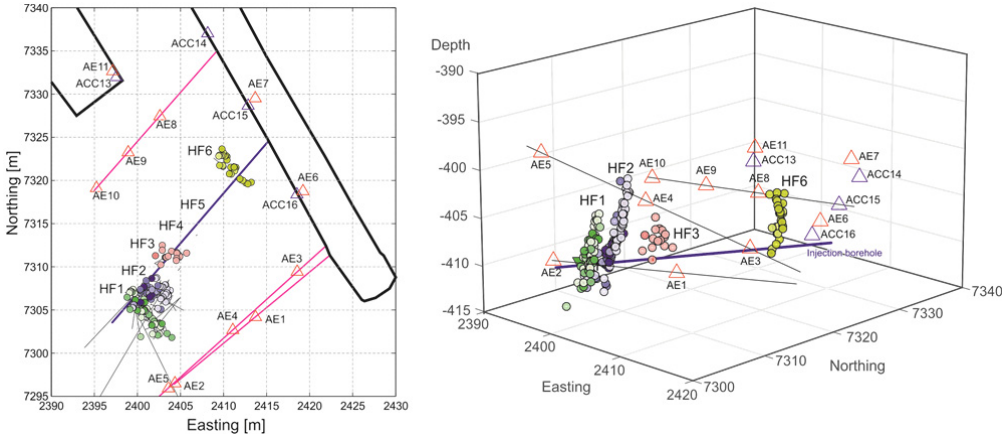

Fig. 3. The map (left) and perspective (right) view of relocated earthquakes observed during all fracture stages HF1-HF6.

To increase the precision of location, the AE activity was relocated using the double-difference relocation technique [10] without waveform cross-correlation. This further improved the quality of location and enabled tracing the spatial and temporal evolution of nano- and picoseismicity in detail. First preliminary results on faulting mechanisms (shear, tensile opening, and compaction) were estimated using polarity data, following the methodology developed for analysis of AE events from laboratory experiments on rock samples [11]. We also manually identified events based on observation of spatial distribution of polarity patterns and calculated the composite fault plane solutions using HASH software [12]. Finally, for selected earthquakes with high signal-to-noise ratio and a sufficient number of clear first P-wave onsets, we calculated the full seismic moment tensors using the hybridMT software package [13, 14].

The waveforms of relatively strong hammer hits, recorded on both high-frequency accelerometers and AE sensors were used to cross-calibrate AE sensors [6, 15] and then calculate moment magnitudes of earthquakes detected during fracturing stages using AE sensors only.

3. First results

All earthquakes detected and relocated in the proximity of the injection borehole occurred during time periods of hydraulic fracturing stages. AEs recorded from each fracture stage are clustered in space and clearly outline the fracture location, its orientation and the temporal evolution of the fracture. For fractures HF1, HF2 and HF3, a clear outward migration of earthquakes away from the injection point is observed. Macroscopically, fractures extend up to 10 m from the horizontal borehole (with HF2 showing the largest extension). The observed macroscopic location and orientation of fractures derived from the AE hypocenter distribution correlate roughly with impression packer results. The calculated composite focal mechanisms of the seismic events typically present one nodal plane almost parallel to the macroscopic fracture plane (Figure 4). The focal mechanisms provide a first constraint on the local stress regime in the area of the experiment (dominance of normal/strike-slip faulting). In general, the seismic moment tensors display dominantly double-couple focal mechanisms with minor contribution of non-double-couple components. Water injection of up to 30 liters (HF2, cf. Table 1 for details) produced seismic events with extremely small moment magnitudes M_W < -4.0 (microfractures of less than cm-size). Finally, the magnitude-frequency distribution of events displays with a b-value b≈1, typical for large earthquakes as well as for acoustic emission experiments in rock samples [14, 16]. We currently investigate characteristic differences in seismic response and source parameters of the seismicity observed in different hydraulic fracturing stages, different formations and injection schemes which will be compared to the injection data and geomechanical parameters of the rocks.

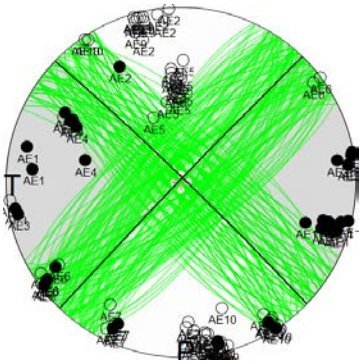

Fig. 4. Example of composite focal mechanism (15 earthquakes) recorded during stage HF2 (uncertainties in green).

Acknowledgements

Nova FoU project 54-14-1 was financially supported by GFZ German Research Center for Geosciences (75%), KIT Karlsruhe Institute of Technology (15%) and Nova Center for University Studies, Research and Development (10%). An additional in-kind contribution of SKB for using Äspö Hard Rock Laboratory as test site for geothermal research is greatly acknowledged. PMG acknowledges funding from the Helmholtz Postdoc Programme.

References

[1] A. Zang, O. Stephansson, L.Stenberg, K. Plenkers, S. Specht, C. Milkereit, E. Schill, G. Kwiatek, G. Dresen, G. Zimmermann, T. Dahm, M. Weber, Hydraulic fracture monitoring in hard rock at 410 m depth with an advanced fluid-injection protocol and extensive sensor array, Geophys. J. Int. 208 (2017) 790–813.

[2] K. Plenkers, D. Schorlemmer, G. Kwiatek, On the Probability of Detecting Picoseismicity, Bull. Seismol. Soc. Am. 101 (2011) 2579–2591.

[3] K. Plenkers, G. Kwiatek, On the Sensitivity of a High-Frequency Acoustic Emission Network, Seismol. Res. Lett. 80 (2009) 344.

[4] G. Manthei, J. Eisenblätter, T. Dahm, Moment tensor evaluation of acoustic emission sources in salt rock, Constr. Build. Mater. 15 (2001) 297–309.

[5] G. Manthei. Characterization of acoustic emission sources in a rock salt specimen under triaxial compression, Bull Seism. Soc Am 95 (2005) 1674–1700.

[6] G. Kwiatek, K. Plenkers, G. Dresen, Source parameters of picoseismicity recorded at Mponeng Deep Gold Mine, South Africa: Implications for scaling relations, Bull. Seismol. Soc. Am. 101 (2011) 2592–2608.

[7] M. Naoi, M. Nakatani, S. Horiuchi, Y. Yabe, J. Philipp, T. Kgarume, G. Morema, S. Khambule, T. Masakale, L. Ribeiro, K. Miyakawa, A. Watanabe, K. Otsuki, H. Moriya, O. Murakami, H. Kawakata, N. Yoshimitsu, A. Ward, R. Durrheim, H. Ogasawara, Frequency–magnitude distribution of $-3.7 \leq Mw \leq 1$ mining-induced earthquakes around a mining front and b-value invariance with post-blast Time, Pure Appl. Geophys. 171 (2014) 2665–2684.

[8] Y. Font, H. Kao, S. Lallemand, C.-S. Liu, L.-Y. Chiao, Hypocentre determination offshore of eastern Taiwan using the Maximum Intersection method, Geophys. J. Int. 158 (2004) 655–675.

[9] A. Lomax, A Reanalysis of the hypocentral location and related observations for the Great 1906 California Earthquake, Bull. Seismol. Soc. Am. 95 (2005) 861–877.

[10] F. Waldhauser, W. L. Ellsworth, A double-difference earthquake location algorithm: Method and application to the Northern Hayward fault, California, Bull. Seismol. Soc. Am. 90 (2000) 1353–1368.

[11] A. Zang, F.W Christian, S. Stanchits, G. Dresen, R. Andresen, A.M. Haidekker, Source analysis of acoustic emissions in Aue granite cores under symmetric and asymmetric compressive loads, Geophys J Int. 135 (1998) 1113–1130.

[12] J. L. Hardebeck, P. M. Shearer, A new method for determining first-motion focal mechanisms. Bull. Seismol. Soc. Am. 92 (2002) 2264.

[13] G. Kwiatek, P. Martínez-Garzón, M. Bohnhoff, HybridMT: A MATLAB/shell environment package for seismic moment tensor inversion and refinement. Seismol. Res. Lett. 87 (2016) 964–976.

[14] G. Kwiatek, T.H.W. Goebel, G. Dresen, Seismic moment tensor and b-value variations over successive seismic cycles in laboratory stick-slip experiments, Geophys. Res. Lett. 41 (2014) 5838–5846.

[15] K. Plenkers, G. Kwiatek, F. Krüger, The AE sensor instrument response in source studies of mining–induced seismicity, in: Proceedings of AGIS Workshop on Induced Seismicity, November 26-28th, Karlsruhe, Germany, 2012.

[16] G. Kwiatek, K. Plenkers, G. Dresen, Frequency-magnitude characteristics down to magnitude -4.4 for induced seismicity recorded at Mponeng gold mine, South Africa, Bull. Seismol. Soc. Am 100 (2010) 1165-1173.